Structural and Functional Characterization of CRAMP-18 Derived from a Cathelicidin-Related Antimicrobial Peptide CRAMP

Kyongsoo Park, Song Yub Shin,† Kyung-Soo Hahm,† and Yangmee Kim*

Department of Chemistry, Konkuk University, Seoul 143-701, Korea
†Department of Bio-Materials, Graduate School and Research Center for Proteineous Materials, Chosun University, Gwangju 501-759, Korea
Received June 23, 2003

CRAMP was identified from a cDNA clone derived from a mouse femoral marrow cells as a member of cathelicidin-derived antimicrobial peptide. Tertiary structure of CRAMP in TFE/H_2O (1 : 1, v/v) solution has been determined by NMR spectroscopy previously and consists of two amphipathic α-helices from Leu4 to Lys10 and from Gly16 to Leu33. These two helices are connected by a flexible region from Gly11 to Gly16. Analysis of series of fragments composed of various portion of CRAMP revealed that an 18-residue fragment with the sequence from Gly16 to Leu33 (CRAMP-18) was found to retain antibacterial activity without cytotoxicity. The effects of two Phe residues at positions 14 and 15 of CRAMP-18 on structure, antibacterial activity, and interaction with lipid membranes were investigated by $Phe^{14,15} \rightarrow Ala$ substitution (CRAMP-18-A) in the present study. Substitution of Phe with Ala in CRAMP-18 caused a significant reduction on antibacterial and membrane-disrupting activities. Tertiary structures of CRAMP-18 in 50% TFE/H_2O (1 : 1, v : v) solution shows amphipathic α-helix, from Glu^2 to Leu^{18}, while CRAMP-18-A has relatively short amphipathic α-helix from Leu^4 to Ala^{15}. These results suggest that the hydrophobic property of Phe^{14} and Phe^{15} in CRAMP-18 is essential for its antibacterial activity, α-helical structure, and interactions with phospholipid membranes.

Key Words : Antimicrobial peptide, CRAMP, CRAMP-18, Phospholipid membranes, Antibacterial activity

Introduction

Two broad classes of mammalian antibimicrobial peptides such as cysteine-rich defensins (α- and β-defensin) and various cathelicidins have been identified.[1-7] Cathelicidins contains an N-terminal domain called cathelin, a putative cysteine-protease inhibitor, and C-terminal domain that comprise an antimicrobial peptide. While the cathelin domains are highly conserved across species, the C-terminal antimicrobial domains are structurally diverse with α-helical, β-sheet, β-turn or extended conformations.[1,6-8] CRAMP is a cathelicidin-related α-helical antimicrobial peptide identified from a cDNA clone isolated from mouse femoral marrow cells.[9] CRAMP exhibits potent antibacterial activity against Gram-positive and Gram-negative bacteria, while has no hemolytic activity against human erythrocytes.[8] CRAMP was known to cause rapid permeabilization of the inner membrane of *Escherichia coli*.[8] Our previous analysis of series of fragments composed of various portion of CRAMP revealed CRAMP from residue 16 to residue 33 with a sequence of GEKLKKIGQKIKNFFQKL (termed as CRAMP-18) is as active as parental CRAMP against Gram-positive and Gram-negative bacterial strains.[10] The tertiary structure of CRAMP in TFE/H_2O (1 : 1, v/v) solution was analyzed by our previous NMR analysis.[11] It was found that CRAMP adopts a unique structure comprising of a N-terminal α-helical region (residues Leu^4-Lys^{10}) and a C-terminal α-helical region (residues Gly^{16}-Leu^{33}) connected by a flexible region from Gly^{11} to Gly^{16}.[11] Therefore, the amphipathic C-terminal α-helical region from Gly^{16} to Leu^{33} of CRAMP can be considered as the functional region that plays an important role in spanning the lipid bilayers as well as its antibacterial activity.

In the present study, to investigate the effects of the two Phe-residues at positions 14 and 15 of CRAMP-18 on structure, antibacterial activity and interaction with lipid membranes, the analogue (CRAMP-18-A) in which Ala is substituted for two Phe-residues in CRAMP-18 was synthesized (Table 1). The antibacterial activity of the peptides against four Gram-negative bacteria and four Gram-positive bacteria was measured. The membrane-interaction ability of the peptides was compared by dye-leakage from the positively charged liposomes. The secondary structures of the peptides in the membrane-mimicking environments such as TFE/H_2O solution, sodium dodecyl sulfate (SDS) micelles and dodecyl phosphocholine (DPC) micelles was measured using CD spectroscopy. The tertiary structures of CRAMP-18 and its analogue in 50% TFE/H_2O (1 : 1, v/v) solution have been determined by two-dimensional NMR spectroscopy.

Experimental Section

Peptide Synthesis. All peptides were synthesized by the solid-phase method using Fmoc-chemistry.[12] The crude peptides were purified by a reversed-phase preparative HPLC

*To whom correspondence should be addressed. Phone: + 82-2-450-3421; Fax: +82-2-447-5987; E-mail: ymkim@konkuk.ac.kr.

on a C_{18} column (20 × 250 mm, Shim-pack) using a linear gradient of 20 to 80% acetonitrile in 0.1% trifluoroacetic acid for 30 min. The correct molecular weights of the synthetic peptides were confirmed by MALDI-TOF mass spectrometry (data not shown).

Antibacterial Activity. *Escherichia coli* (KCTC 1637) and *B. subtilis* (KCTC 3068) were purchased from the Korea Collection for Type Cultures (KCTC), Korea Research Institute of Bioscience & Biotechnology (KRIBB) (Taejon, Korea). The bacteria were grown the mid-logarithmic phase in LB medium (1% tryptone, 0.5% yeast extract and 1% NaCl). Antimicrobial activities of the peptides were measured by colony account assay. Mid-logarithmic phase bacteria (1×10^6 CFU/mL) were incubated with the peptide concentration of 6 μM in 1% peptone, and aliquots were drawn out at different intervals after incubation and were plated on LB broth agar. The number of colonies developed was determined after incubating the plates for 18 h at 37 °C.

Circular Dichroism (CD). CD spectra of the peptides were recorded using a Jasco J-720 spectropolarimeter (Japan Spectroscopic Co. Tokyo). Four scans per sample were performed over wavelength range 190-250 nm at 0.1 nm intervals. The CD spectra of the peptides in H_2O, 50% TFE/H_2O (v/v) solution, 100 mM SDS micelles and 10 mM DPC micelles were measured at 25 °C using a 1 mm path-length cell. The mean residue ellipticity, [θ], is given in deg·cm^2·dmol^{-1}.

Peptide-induced Leakage from Calcein-loaded Liposomes. Small unilamellar vesicles (SUVs) composed of POPC (1-palmitoyl-2-oleoylphosphatidylcholine)/POPG (1-palmitoyl-2-oleoylphosphatidylglycerol) (3 : 1, w/w) were prepared for dye-leakage experiment as follow. Phospholipid (7.5 mg) was dissolved in chloroform and dried with a stream of nitrogen to form a thin lipid film on the wall of a glass tube. The lipid concentration was 0.5 mM. The dried lipid was hydrated with 2 mL of Tris-HCl buffer [10 mM Tris-HCl (pH 7.4)/154 mM NaCl/0.1 mM EDTA] containing 70 mM calcein. The suspension was vortex-mixed for 10 min. The resultant lipid dispersions were then sonicated in ice water for 20-30 min with a titanium-tipped sonicator until clear. Calcein-entrapped vesicles were separated from free calcein by gel filtration using Sephadex G-50 column with the same buffer. To Tris-HCl buffer (pH 7.4, 2 mL) in a cuvette was added to 20 μL of the vesicles containing 70 mM calcein to give a vesicle solution with a final concentration of 70 μM lipid. To a cuvette placed in a holder (25 °C) was added 20 μL of an appropriate dilution of the peptides in the buffer. The fluorescence intensities of calcein released from liposomes were monitored at 520 nm (excited at 490 nm) on a Jasco FP-750 spectrofluorimeter (Tokyo, Japan) and measured 2 min after the addition of the peptides. To measure the fluorescence intensity for 100% dye-leakage, 20 μL of Triton-X100 (20% in Tris-HCl buffer) was added to dissolve the vesicles. The percentage of dye-leakage caused by the peptides was calculated using the following equation: % leakage = $100 \times (F-F^0)/(F^t-F^0)$, where F^0 and F^t are the initial fluorescence intensities observed without the peptides and after Triton X-100 treatment, respectively and F is the fluorescence intensity achieved by the peptides.

NMR Experiment. Samples for NMR experiments were dissolved in 50% TFE/H_2O (1 : 1, v/v) solution. Resonances of CRAMP in other membrane-mimicking environment such as SDS micelle and DPC micelle were too broad to be assigned completely. Concentration of the samples was 1.0 mM. All of the phase-sensitive two-dimensional experiments, such as DQF-COSY, TOCSY, and NOESY were performed using time-proportional phase incrementation method.[13-17] TOCSY experiments were performed using 20, 40, and 80 ms MLEV-17 spin-lock mixing pulses. Mixing times of 150, 250, and, 350 ms were used for NOESY experiments. $^3J_{HN\alpha}$ coupling constants were measured from DQF-COSY spectrum with a spectral width of 4006.41 Hz and digital resolution of 0.98 Hz/point.[18] Chemical shifts are expressed relative to DSS signal at 0 ppm. All the spectra were recorded at 277, 288, 298 and 308 on Bruker 400 MHz DPX-spectrometer at Konkuk University and Varian 500 MHz NMR spectrometer at KBSI. Temperature coefficients were calculated from the TOCSY experiments at three different temperatures (288, 298, and 308 K) to investigate the intramolecular hydrogen bondings in the peptides.[19] NMR spectroscopy can give useful information about the interaction between the peptides and micelles. NOESY experiments for the sample in non-deuterated SDS micelles was executed at 298 K with mixing times of 250 and 600 ms. All NMR spectra were processed off-line using the FELIX software package on SGI (Molecular Simulations Inc., San Diego, CA, USA).

Structure Calculation. Distance constraints were extracted from the NOESY spectra with mixing times of 150 and 250 ms. The volumes of the NOEs between the two protons of Phe residues were used as references. All other volumes were converted into the distances by assuming a simple $1/r^6$ distance dependence. All the NOE intensities are divided into three classes (strong, medium, and weak) with distance ranges of 1.8-2.7, 1.8-3.3, and 1.8-5.0 Å, respectively.[20,21] Structure calculations were carried out using X-PLOR version 3.851.[22] with the topology and parameter sets topallhdg and parallhdg, respectively. Standard pseudoatom corrections were applied to the nonstereospecifically assigned restraints.[23] and an additional 0.5Å was added to the upper bounds for the NOEs involving methyl protons.[24] A hybrid distance geometry-dynamical simulated annealing protocol[25,26] was employed to generate the structures. Total of 80 structures were generated, 20 structures with the lowest energies were selected for the further analysis.

Table 1. Amino acid sequences of CRAMP, CRAMP-18 and CRAMP-18-A

Peptide	Sequence
CRAMP	ISRLAGLLRKGGEKIGEKLKKIGQKIKNFFQK LVPQPE
CRAMP-18	GEKLKKIGQKIKNFFQKL
CRAMP-18-A	GEKLKKIGQKIKNAAQKL

Results and Discussion

Antibacterial and Membrane-Disrupting Activities. The antibacterial activity of the peptides was determined by the colony count assay in *E. coli* and *B. subtilis*. As shown in Figure 1, the substitution (CRAMP-18-A) of Phe[14,15] with Ala in CRAMP-18 induced a remarkable reduction on antibacterial activities against *E. coli* and *B. subtilis*. The peptide-induced membrane disrupting activity was examined on the basis of the leakage of the fluorescent dye calcein from SUVs composed of POPC/POPG (3 : 1, w/w). Figure 2 shows the true percent leakage value according to the peptide concentration. CRAMP-18-A was found to show much weaker membrane disrupting activity than that of CRAMP-18.

Circular Dichroism Study. To investigate the secondary structures of CRAMP-18 and CRAMP-18-A in membrane mimetic environments, CD spectra were measured in aqueous buffer, TFE/water solution, SDS micelles, and DPC micelles. As shown in Figure 3, CRAMP-18 and CRAMP-18-A had a random coil structure in the water. However,

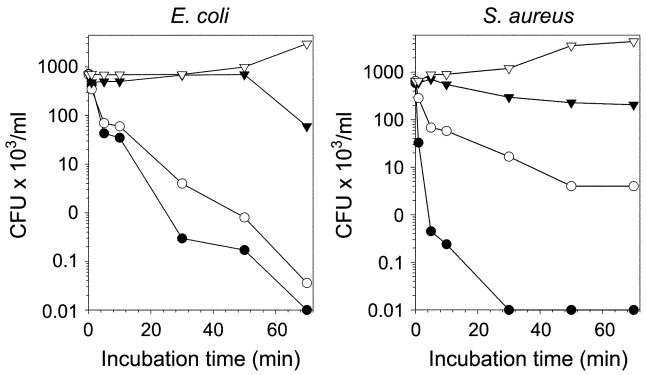

Figure 1. Antibacterial activities of the peptides in colony count assay; CRAMP (●); CRAMP-18 (○); CRAMP-18-A (▼); No peptide (▽).

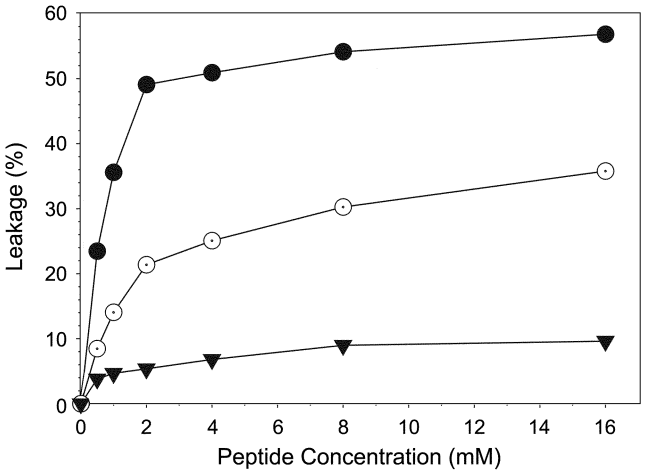

Figure 2. Leakage of the fluorescent probe calcein from POPC/POPG (3 : 1, w/w) liposomes is defined as the percent leakage after 5 min at a lipid concentration of 70 μM; CRAMP (●); CRAMP-18 (○); CRAMP-18-A (▼).

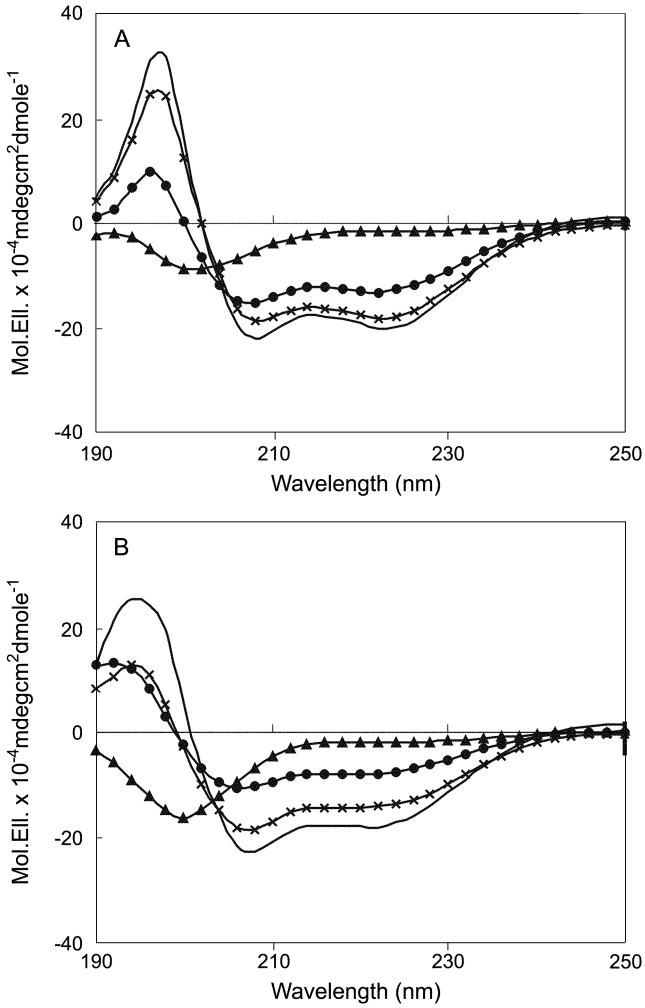

Figure 3. Circular dichroism spectra of (A) CRAMP-18 and (B) CRAMP-18-A in H_2O (– ▲ –), 50% TFE/ H_2O solution (– ● –), 10 mM DPC micelles (– × –) and 100 mM SDS micelles (—).

CRAMP-18 and CRAMP-18-A in TFE/water solution, SDS micelles, and DPC micelles adopt α-helical conformations in membrane-mimicking environments. As shown in Figure 3, the content of α-helix in CRAMP-18 was higher than CRAMP-18-A in TFE/H_2O solution, SDS micelles and DPC micelles.

Resonance Assignment and Secondary Structure. Sequence specific resonance assignment was determined using mainly DQF-COSY, TOCSY and NOESY data.[27] Figure 4 shows the NOESY spectra with the sequential assignments of CRAMP-18 and CRAMP-18-A in the NH-NH region. NOESY and TOCSY experiments at 277, 288, 298 and 308 K allowed the complete assignment of the overlapping peaks. Chemical shifts of CRAMP-18 and CRAMP-18-A in DPC micelle at 288 K, referenced to DSS, are listed in Tables 2.

The observation of sequential $d_{NN}(i,i+1)$ and medium range $d_{\alpha\beta}(i,i+3)$, $d_{\alpha N}(i,i+3)$ and $d_{\alpha N}(i,i+4)$ NOEs strongly supports the presence of α-helix spanning residues from Glu[2] to Leu[18] in CRAMP-18 and from Leu[4] to Ala[15] in CRAMP-18-A. The observed values of the $^3J_{HN\alpha}$ coupling

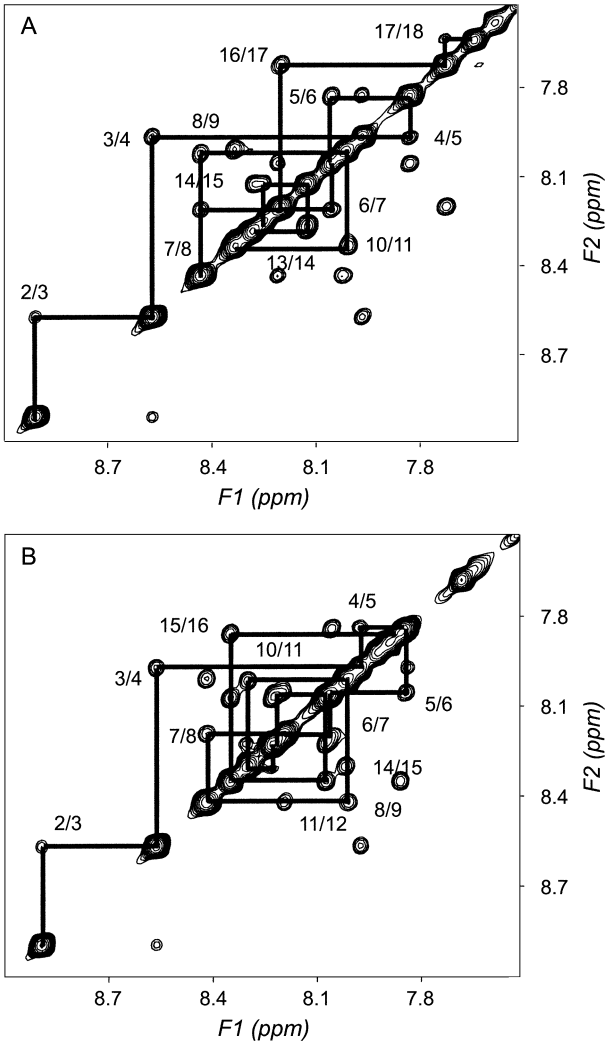

Figure 4. NH-NH region of a 250 ms mixing time NOESY spectrum of (A) CRAMP-18 and (B) CRAMP-18-A.

constants for the helical region of CRAMP-18 and CRAMP-18-A are generally below 6 Hz and they are marked with reversed triangles as shown in Figure 5. The values of the amide proton temperature coefficient have been used to predict hydrogen bond donors and values more positive than -4.5 ppb/K can be taken as an indicator that the amide proton is involved in intramolecular hydrogen bonding.[28] As shown in Figure 5, temperature coefficients of many amide protons of CRAMP-18 and CRAMP-18-A are generally more positive than -4.5 ppb/K and this result indicates that these peptides have an α-helical structure. A dense grouping of four or more -1 values of chemical shift indices not interrupted by a +1 in these regions indicates the presence of an α-helix.[29] The presence of small $^3J_{HN\alpha}$ coupling constants, the sequence of residues with chemical shift indices of -1, temperature coefficients, and the NOE patterns present strong evidences that CRAMP-18 and CRAMP-18-A in TFE/H_2O (1 : 1, v:v) solution have an α-helical structure.

Tertiary Structures of CRAMP-18 and CRAMP-18-A. To determine the tertiary structures of CRAMP-18 and CRAMP-18-A, we used experimental restraints such as

Table 2. ^{1}H chemical shift (ppm) for (A) CRAMP-18 and (B) CRAMP-18-A in TFE/H_2O (1 : 1, v/v) solution at 288 K

A

Residue	NH	αH	βH	Others
^{1}Gly				
^{2}Glu	8.90	4.35	2.16, 2.12	γ 2.50*
^{3}Lys	8.57	4.09	1.89*	γ 1.45*; δ 1.57*; ε 3.01*
^{4}Leu	7.96	4.22	1.71*	δ_1 0.98*, δ_2 0.93*
^{5}Lys	7.82	4.12	1.94*	γ 1.49*; δ 1.60*; ε 3.02*
^{6}Lys	8.05	4.19	2.04*	γ 1.51*; δ 1.75, 1.65; ε 3.02*
^{7}Ile	8.20	3.85	1.98	γ_1 1.77, 1.20; γ_2 0.98*; δ 0.89*
^{8}Gly	8.43	3.86*		
^{9}Gln	8.02	4.11	2.29, 2.23	γ 2.55, 2.46; δ 7.49, 6.87
^{10}Lys	8.01	4.13	2.10*	γ 1.51*; δ 1.75 1.66, ε 3.01*
^{11}Ile	8.33	3.86	2.01	γ_1 1.83, 1.18; γ_2 1.06*; δ 0.88*
^{12}Lys	8.28	4.12	1.98*	γ 1.50*; δ 1.64*; ε 3.01*
^{13}Asn	8.27	4.54	2.99, 2.84	γ 7.64, 6.86
^{14}Phe	8.12	4.29	3.23, 3.17	2,6H 6.79; 3,5H 7.20
^{15}Phe	8.25	4.31	3.30, 3.09	2,6H 7.26; 3,5H 7.33
^{16}Gln	8.19	4.24	2.27, 2.22	γ 2.58, 2.47; δ 7.48, 6.75
^{17}Lys	7.72	4.33	1.94, 1.84	γ 1.53*; ε 3.02*
^{18}Leu	7.64	4.32	1.63*	δ_1 0.86*, δ_2 0.80*

[a]Chemical shifts are relative to DSS at 0 ppm.

B

Residue	NH	αH	βH	Others
^{1}Gly				
^{2}Glu	8.89	4.34	2.16, 2.12	γ 2.49*
^{3}Lys	8.56	4.10	1.89*	ε 3.01*
^{4}Leu	7.96	4.22	1.70*	δ_1 0.97*, δ_2 0.94*
^{5}Lys	7.83	4.12	1.93*	γ 1.45*; δ 1.58*; ε 3.02*
^{6}Lys	8.05	4.18	2.01*	γ 1.51*; δ 1.75, 1.65; ε 3.02*
^{7}Ile	8.19	3.86	1.98	γ 1.75, 1.21; γ 0.98*; δ 0.90*
^{8}Gly	8.41	3.86*		
^{9}Gln	8.00	4.11	2.27, 2.20	γ 2.53, 2.45; δ 7.49, 6.86
^{10}Lys	8.01	4.14	2.09*	ε 3.01*
^{11}Ile	8.30	3.82	1.96	$\gamma_1$1.79, 1.16; γ_2 1.06*; δ 0.86*
^{12}Lys	8.22	4.05	1.94*	γ 1.57*; δ 1.46*; ε 3.01*
^{13}Asn	8.22	4.56	2.95, 2.88	γ 7.87, 6.86
^{14}Ala	8.06	4.23	1.56*	
^{15}Ala	8.35	4.32	1.52*	
^{16}Gln	7.87	4.27	2.27, 2.17	γ 2.56, 2.48; δ 7.48, 6.76
^{17}Lys	7.92	4.38	1.98, 1.89	γ 1.54*; ε 3.02*
^{18}Leu	7.88	4.41	1.76*	δ_1 0.94*, δ_2 0.88 *

[a]Chemical shifts are relative to DSS at 0 ppm.

sequential ($|i-j|=1$), medium-range ($1<|ij|\leq 5$), long-range ($|i-j|>5$), intraresidual distance, and torsion angle restraints, as listed in Table 3. From the structures, which were accepted with a small deviations from idealized covalent geometry and experimental restraints (≤ 0.05 Å for bonds, ≤ 5° for angles, ≤ 5° for chirality, ≤ 0.3 Å for NOE restraints, and ≤ 3° for torsion angle restraints), and 20 output structures with the lowest energy for each peptides were analyzed.

The statistics of the 20 final simulated annealing (SA)

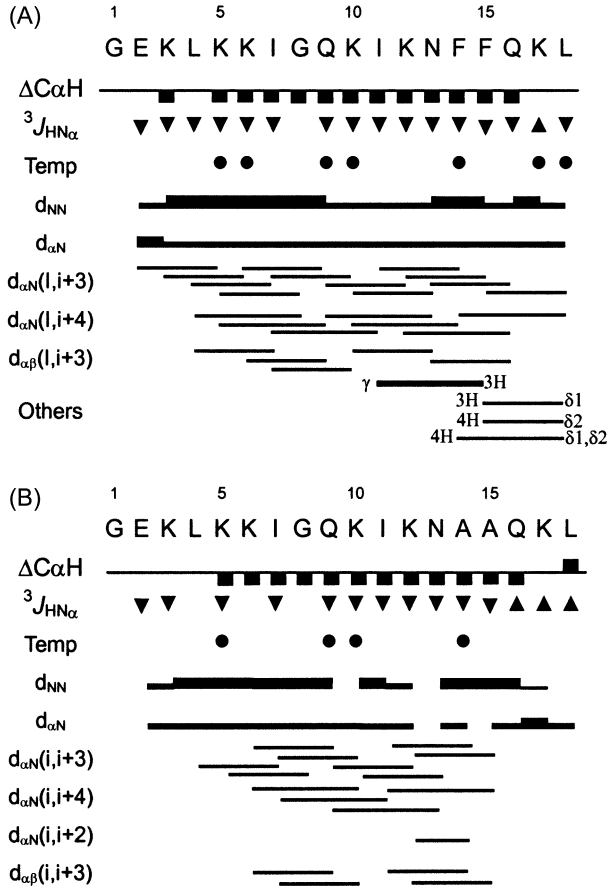

Figure 5. Summary of the NOE connectivities, CSI values, temperature coefficients more positive than -4.5 ppb/K, and coupling constants for (A) CRAMP-18 and (B) CRAMP-18-A in TFE/H_2O (1 : 1, v/v) solution. Line thickness for the NOEs reflects the intensity of the NOE connectivities.

structures of CRAMP-18 and CRAMP-18-A are given in Table 3. The overall convergence of the final set of structures can be quantified by atomic rmsd values. When we superimposed the 20 structures on the backbone atoms (N, Cα, C', O) of the residues from Glu[2] to Leu[18] in the CRAMP-18 and from Leu[4] to Ala[15] in the CRAMP-18-A. Rmsd from mean structure for CRAMP-18 were 0.48 Å for the backbones atoms and 1.12 Å for all heavy atoms and those for CRAMP-18-A were 0.31 Å and 1.04 Å, respectively.

Figure 6 shows the superposition of 20 lowest energy structures on the backbone atoms and they converge to an α-helical structure of CRAMP-18 and CRAMP-18-A in TFE/H_2O (1 : 1, v,v) solution. This shows clearly that CRAMP-18 has an α-helical structure of about four turns from Glu[2] to Leu[18], CRAMP-18-A has relatively short α-helix from Leu[4] to Ala[15] .

Structure-Activity Relationships. Many of the known antimicrobial properties have been postulated as arising from bacterial membranes through the formation of ion channels. In order to form an ion channel, a bundle of at least three or four membrane-spanning helices forms an ion channel with the polar side chains oriented toward the bundle center. The amphipathic α-helix is a critical component in

Table 3. Structural Statistics and Mean Pairwise rmsds for the 20 lowest Structures of CRAMP-18 and CRAMP-18-A in TFE/H_2O (1 : 1, v/v) solution[a]

	CRAMP-18	CRAMP-18-A
Experimental distance restraints		
Total	186	128
Sequential	59	50
Medium range	35	21
Intraresidue	92	57
Dihedral angle restraints	15	14
Rmsd from experimental restraints		
NOE (Å)	0.051 ± 0.001	0.036 ± 0.001
ϕ (deg)	0.260 ± 0.049	0.174 ± 0.062
Rmsd from convalent geometry		
Bonds (Å)	0.003 ± 0.0001	0.002 ± 0.0001
Angles (deg)	0.523 ± 0.006	0.491 ± 0.003
Impropers (deg)	0.427 ± 0.010	0.420 ± 0.006
Average energies (kcal mol^{-1})		
E_{tot}	61.4 ± 1.00	34.6 ± 0.72
E_{NOE}	25.6 ± 1.38	8.57 ± 0.54
E_{tor}	25.3 ± 0.57	20.9 ± 0.22
E_{repel}	2.04 ±0.50	0.09 ± 0.03
Rmsd from the mean structure		
Backbone atoms of all residues	0.56 ± 0.17	0.92 ± 0.31
All heavy atoms of all residues	1.13 ± 0.15	1.71 ± 0.33
Backbone atoms of C-terminal residues	0.48 ± 0.14 (2-18)	0.31 ± 0.09 (4-15)
All heavy atoms of C-terminal residues	1.12 ± 0.14 (2-18)	1.04 ± 0.11 (4-15)

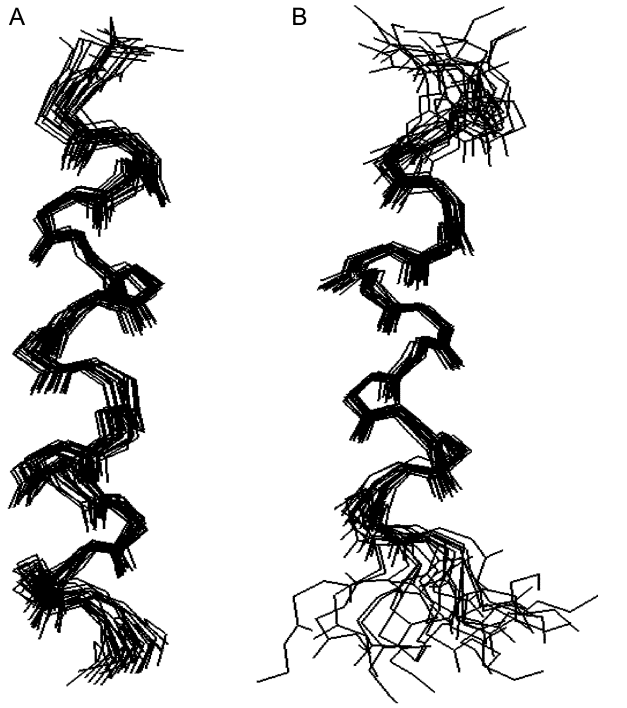

Figure 6. The superpositions of 20 lowest energy structures of (A) CRAMP-18 on the backbone atoms of residue from Glu[2] to Leu[18] and (B) CRAMP-18-A from Leu[4] to Ala[15] in TFE/H_2O (1 : 1, v/v) solution.

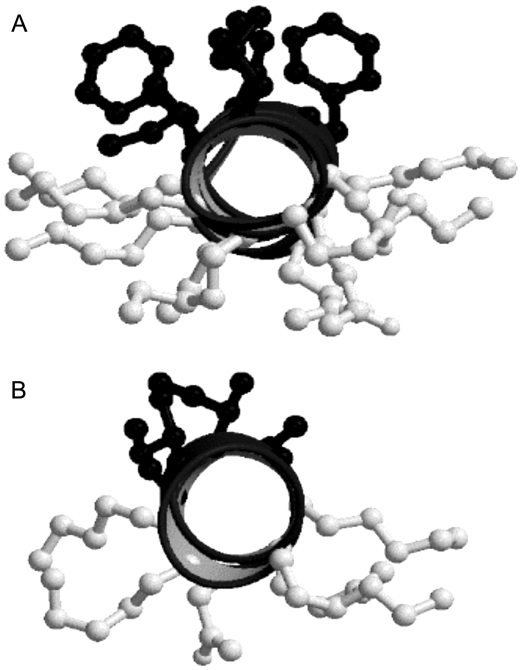

Figure 7. End-on view of the restrained minimized mean structure of (A) CRAMP-18 from Glu[2] to Leu[18] and (B) CRAMP-18-A from Glu[4] to Ala[15] as seen along the α-helix in TFE/ H_2O (1 : 1, v:v) solutions. The hydrophobic side chains are dictated with black color, while the hydrophilic side chains are dictated with gray color.

the pore formation of ion channels. The tertiary structures of CRAMP-18 shows that all of the hydrophobic side chains protrude toward one side, while the positively charged side chains protrude toward the other side as shown in Figure 7. We can suppose that CRAMP-18 possesses an antimicrobial properties, of which the hydrophobic residues of CRAMP-18 interact with the acyl chains of the lipid bilayer while the positively charged side chains of Lys residues are exposed to the aqueous environments if CRAMP-18 makes the ion channels.

According to the tertiary structure, CRAMP-18 has an amphipathic α-helix, from Glu[2] to Leu[18], while CRAMP-18-A has relatively short amphipathic α-helix, from Leu[4] to Ala[15]. A Phe[14,15] $\rightarrow$ Ala substitution in CRAMP-18-A resulted in significant reduction on antibacterial activity and liposome-disrupting activity as compared to CRAMP-18. Because Ala[14] and Ala[15] residues which result in a shorter α-helix in CRAMP-18-A couldn't make effective interaction with membrane, CRAMP-18-A doesn't have effective antibacterial activities.

Interactions between CRAMP-18 and SDS Micelles. NMR spectroscopy has been used to investigate the structures of peptides and the interactions between membrane and peptides.[30-32] More detailed interactions between CRAMP-18 and micelles were investigated by NOESY experiments in non-deuterated SDS micelles as shown in Figure 8. As shown in this figure, aromatic ring protons of Phe[14] and Phe[15] are in contact with methylene protons of SDS micelles. The side chain atoms of these aromatic residues may have close contacts with the hydrophobic acyl chains of micelles. Since

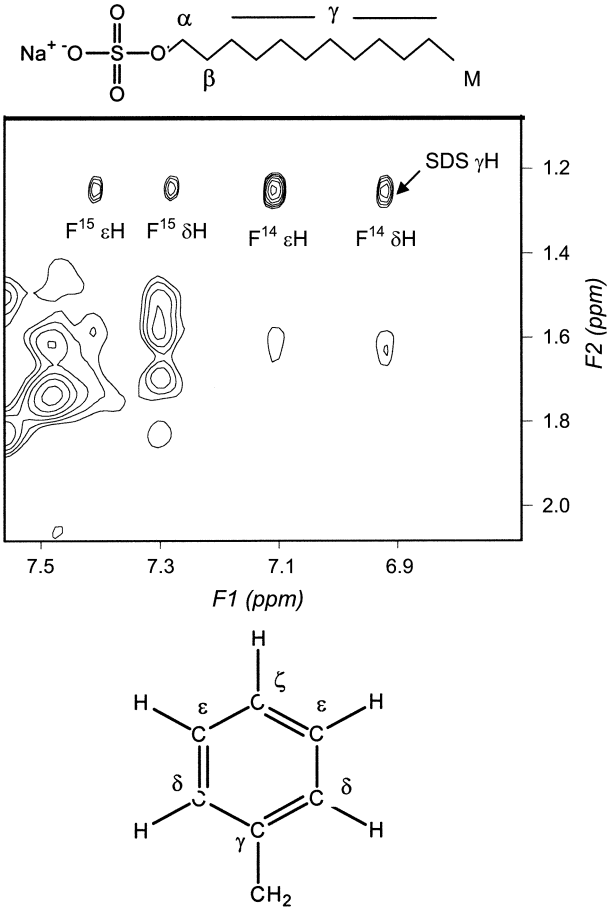

Figure 8. NOESY spectrum of CRAMP-18 in 30 mM SDS micelles recorded with a mixing time of 250 msec. NOE contacts between the aromatic rung protons of Phe[14], Phe[15] and methylene proton of SDS are indicated. Naming schemes for the atoms in SDS and Phenylalanine are shown, too.

resonances of methylene protons of SDS are the average of the 18 methylene protons of SDS, the accurate position of contacts can not be estimated from NOEs. NOEs involving methyl or α-protons of SDS micelles were not observed. These results imply that the hydrophobic property of Phe[14] and Phe[15] in CRAMP-18 may play an important role on its folding and antibiotic activity.

Conclusion

Tertiary structures of CRAMP-18 in 50% TFE/H_2O (1 : 1, v:v) solution shows amphipathic α-helix, from Glu[2] to Leu[18], while CRAMP-18-A has relatively short amphipathic α-helix from Leu[4] to Ala[15]. CRAMP-18 displays good lytic activities against Gram-positive and Gram-negative bacteria, but have no hemolytic activities against human erythrocytes while CRAMP-18-A has a significantly lower antibacterial and membrane-disrupting activities than CRAMP-18. In the red blood cell membrane, the distribution of lipids in the two leaflets is such that the zwitterionic phospholipids, such as phosphatidylcholine and sphingomyelin, are mostly present in the outer leaflet of the bilayer, while the negatively-

charged phosphatidylserine is present exclusively in the inner leaflet. Therefore, the hydrophobicity of the peptide is crucial for the hemolytic activities. However, in the case of bacterial cells, the negatively-charged phosphatidylserine is present exclusively in the outer leaflet. Therefore, peptides with positively charged residues show strong lytic activity against bacterial cells. CRAMP-18 has six positively charged Lys residues and has potent antibacterial activity without cytotoxicity.

It can be concluded that the hydrophobic interaction of Phe rings in CRAMP with the membrane may be important in stabilizing the helical secondary structure of CRAMP. Strong electrostatic interactions between the positively charged Lys residues of CRAMP-18 and the negatively charged phospholipid head groups may be the primary factor for CRAMP-18 binding to the cell membrane. Then, the immersion into the hydrophobic core of the lipid bilayers by the amphipathic α-helical structure of CRAMP-18 and hydrophobic interactions between Phe residues in CRAMP-18 and the acyl chains of the phospholipid may lead to membrane lysis. These structural features of CRAMP-18 are essential for its antibiotic activity and interaction with membrane. Study of the structure-antibiotic activity of these peptides would be helpful for designing ideal antimicrobial peptides with potent antibiotic activity against bacterial, fungal, and tumor cells without lytic activity against erythrocytes and normal mammalian cells.

Acknowledgment. This study was supported by the grant of the Ministry of Science and Technology, Korea and the Korea Science and Engineering Foundation through the Research Center for Proteineous Materials. Yangmee Kim was supported by Konkuk University in 2002.

References

1. Zaiou, M.; Gallo, R. L. *J. Mol. Med.* **2002**, *80*, 549.
2. Boman, H. G. *Scand. J. Immunol.* **1998**, *48*, 15.
3. Lehrer, R. I.; Ganz, T. *Curr. Opin. Immunol.* **1999**, *11*, 23.
4. Maloy, W. L.; Kari, U. P. *Biopolymers* **1995**, *37*, 105.
5. Martin, E.; Ganz, T.; Lehrer, R. I. *J. Leukoc. Biol.* **1995**, *58*, 128.
6. Zanetti, M.; Gennaro, R.; Romeo, D. *Ann. N. Y. Acad. Sci.* **1997**, *832*, 147.
7. Zanetti, M.; Gennaro, R.; Romeo, D. *FEBS Lett.* **1995**, *374*, 1.
8. Gennaro, R.; Zanetti, M. *Biopolymers* **2000**, *55*, 31.
9. Gallo, R. L.; Kim, K. J. *J. Biol. Chem.* **1997**, *272*, 13088.
10. Ha, J. M.; Shin, S. Y.; Kang, S. W. *Bull. Korean Chem. Soc.* **1999**, *20*, 1073.
11. Yu, K.; Park, K.; Kang, S. W.; Shin, S. Y.; Hahm, K. S.; Kim, Y. *J. Pept. Res.* **2002**, *60*, 1.
12. Atherton, E.; Logan, C. J.; Sheppard, R. C. *J. Chem. Soc. Perkin. Trans. I* **1981**, *20*, 538.
13. Derome, A.; Williamson, M. *J. Magn. Reson.* **1990**, *88*, 177.
14. Bax, A.; Davis, D. G. *J. Magn. Reson.* **1985**, *65*, 355.
15. Macura, S.; Ernst, R. R. *Mol. Phys.* **1980**, *41*, 95.
16. Bax, A.; Davis, D. G. *J. Magn. Reson.* **1985**, *63*, 207.
17. Marion, D.; Wüthrich, K. *Biochem. Biophys. Res. Commun.* **1983**, *113*, 967.
18. Kim, Y.; Prestegard, J. P. *J. Magn. Reson.* **1989**, *84*, 9.
19. Hicks, R. P.; Beard, D. J.; Young, J. K. *Biopolymers* **1992**, *32*, 85.
20. Clore, G. M.; Gronenborn, A. M. *CRC Crit. Rev. Biochem. Mol. Biol.* **1989**, *24*, 479.
21. Clore, G. M.; Gronenborn, A. M. *Protein Sci.* **1994**, *3*, 372.
22. Brünger A.T. *X-PLOR Manual, Version 3.1*; Yale University: New Haven, CT, 1993.
23. Wüthrich, K.; Billeter, M.; Braun, W. *J. Mol. Biol.* **1983**, *169*, 949.
24. Clore, G. M.; Gronenborn, A. M.; Nilges, M.; Ryan, C. A. *Biochemistry* **1987**, *26*, 8012.
25. Nilges, M.; Clore, G. M.; Gronenborn, A. M. *FEBS Lett.* **1988**, *229*, 317.
26. Kuszewski, J.; Nilges, M.; Brünger, A. T. *J. Biomol. NMR* **1992**, *2*, 33.
27. Wüthrich, K. *NMR of Protein and Nucleic Acid*; Wiley-Interscience: New York, 1986.
28. Baxter, N. J.; Williamson, M. P. *J. Biomol. NMR* **1997**, *9*, 359.
29. Wishart, D. S.; Sykes, B. D.; Richards, F. M. *Biochemistry* **1992**, *31*, 1647.
30. Bang, E.; Lee, C.; Yoon, J.; Chung, J.; Lee, D.; Lee, W. *Bull. Korean Chem. Soc.* **2001**, *2*(5), 507.
31. Yu, K.; Kang, S.; Kim, S.; Ryu, P.; Kim, Y. *Journal of Biomolecular Structure and Dynamics* **2001**, *18*(4), 595.
32. Park, K.; Baek, D.; Lim, D.; Park, S.; Kim, M.; Park, Y.; Kim, Y. *Bull. Korean Chem. Soc.* **2001**, *22*, 984.